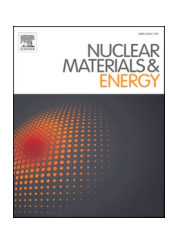
ELSEVIER

Contents lists available at ScienceDirect

### **Nuclear Materials and Energy**

journal homepage: www.elsevier.com/locate/nme



## Interaction of light ions with plasma-facing materials: Improved experimental accuracy and its impact on sputter yield simulations<sup>★</sup>

E. Pitthan <sup>a,1,\*</sup>, M. Fellinger <sup>b,1</sup>, B.Burazor Domazet <sup>b</sup>, P.M. Wolf <sup>a</sup>, J. Shams-Latifi <sup>a</sup>, F. Aumayr <sup>b</sup>, D. Primetzhofer <sup>a</sup>

#### ARTICLE INFO

# Keywords: Ion–solid interaction Plasma-facing materials Sputtering yields Stopping power Interatomic potential Ion beam analysis

#### ABSTRACT

This work investigates how corrections to fundamental parameters describing ion—solid interaction affect sputtering yield simulations based on the binary collision approximation. We review recent experimental assessments of electronic stopping power and short-range repulsive interatomic potentials for light plasma species (H, D, He) in plasma-facing material candidates (W, Fe, EUROFER97), and compare them to widely used semi-empirical and theoretical models. At low energies, discrepancies of up to 60% relative to SRIM-2013 and up to 210% relative to SRIM-1997 are identified for the specific energy loss, highlighting the need for improved input parameters. We assess the sensitivity of sputtering yields to these corrections using SDTrimSP simulations, and compare the results to new experimental sputter yield data obtained for re-deposited thin W, Fe, and EUROFER97 films on a high-sensitivity quartz crystal microbalance. Incorporating derived stopping powers and interatomic potentials into the simulation significantly reduces the discrepancies between experimental and simulated sputtering yields. Remaining uncertainties and model limitations, such as crystal structure effects and ion implantation, are discussed.

#### 1. Introduction

Understanding plasma-wall interactions (PWI) is essential for the operation and longevity of plasma-facing materials (PFM) in fusion reactors. The extreme conditions in fusion devices, characterized by high particle fluxes, thermal loads, and material erosion, necessitate accurate modeling to predict material response and guide the selection of optimal PFM [1–3]. Sputtering, defect formation, and hydrogen isotope retention are key processes that influence reactor performance, and their accurate modelling depends on reliable knowledge of fundamental quantities describing ion–solid interaction such as electronic stopping power, and nuclear interactions described by interatomic potentials [4–6].

Sputtering yields (SY), defined as the average number of atoms ejected per incoming particle, quantify the erosion of PFM by plasma particles and their subsequent contamination of the plasma or redeposition of PFM elsewhere in the reactor [7–10]. Models for SY

simulations, including those based on the binary collision approximation (BCA) and molecular dynamics (MD), rely on semi-empirical or abinitio derived interaction potentials and stopping power formulations [11–14]. However, experimental validation of these input parameters remains limited, particularly for slow, light ions (H, D, He) in PFM such as tungsten (W), a candidate first-wall material for future fusion reactors [3,15], and structural materials such as EUROFER97 [16].

In this work, we review the current status of two key quantities that describe ion–solid interaction: (i) The energy depositions via inelastic collisions between the ion and the target material, characterized by the electronic stopping power (energy loss per unity path), or alternatively, the stopping cross section (SCS), which normalized the stopping power by the atomic density of the target, to remove the trivial dependence on material density; (ii) Repulsive interatomic potentials, which directly affect interaction cross sections, and thus determine the energy and angle distribution of scattered and recoiling particles in the collision cascade responsible for physical sputtering. Recent studies have

<sup>&</sup>lt;sup>a</sup> Department of Physics and Astronomy, Ångström Laboratory, Uppsala University, Box 516, SE-751 20 Uppsala, Sweden

<sup>&</sup>lt;sup>b</sup> Institute of Applied Physics, TU Wien, Fusion@ÖAW, Wiedner Hauptstraβe 8-10/E134, A-1040 Vienna, Austria

<sup>\*</sup> This article is part of a special issue entitled: 'PFMC-20' published in Nuclear Materials and Energy.

<sup>\*</sup> Corresponding author at: Department of Physics and Astronomy, Ångström Laboratory, Uppsala University, Box 516, SE-751 20 Uppsala, Sweden. E-mail address: eduardo.pitthan@physics.uu.se (E. Pitthan).

 $<sup>^{1}</sup>$  Contributed equally to this work.

revealed discrepancies of up to 60 % between semi-empirical models and experimental results for electronic SCS at low energies [17], highlighting the need for improved datasets. Inaccuracies in stopping power and interaction potentials can propagate through PWI models, affecting predicted sputtering yields, implantation depths, and defect generation.

Beyond their role in PWI modeling, SCS and interatomic potentials are also critical for ex-situ analysis of reactor components. Ion beam analysis (IBA) techniques, such as Rutherford Backscattering Spectrometry (RBS), Elastic Recoil Detection Analysis (ERDA) and Nuclear Reaction Analysis (NRA), are widely used to quantify impurity deposition, fuel retention, and material modification in exposed PFM [18–20]. The accuracy of these techniques depends on reliable knowledge of energy loss mechanisms and cross-sections, which are governed by stopping power and interatomic potentials. Inaccuracies in these fundamental quantities introduce uncertainties in depth profiling and compositional analysis, limiting the precision of fusion material assessments. Therefore, improving the experimental understanding of these parameters is essential for both predictive PWI simulations and diagnostic techniques in fusion research.

To address these issues, we review recent experimental investigations of energy depositions and interaction potentials for light ions in key PFM: W, EUROFER97, and iron (Fe), as the main component of EUROFER97 and steels. We quantify deviations from commonly used semi-empirical and theoretical models, with focus on fusion-relevant ion energies, i.e. below 10 keV. The experimental results are integrated into BCA-based simulations using the SDTrimSP code [12] to assess their impact on predicted sputtering yields. Finally, simulated sputtering yields containing experimentally corrected stopping power and interatomic potentials are directly compared to newly obtained experimental yield data using thin films of PFM (W, Fe, and EUROFER97) deposited on a high-sensitivity quartz crystal microbalance (QCM) [21]. The incorporation of corrected stopping powers and interatomic potentials into the simulations significantly improves agreement between simulated and experimental sputtering yields for all studied cases. Remaining sources of uncertainty, such as crystallinity effects are also discussed.

#### 2. Materials and methods

For the experimental measurements of sputtering yields using a high-sensitivity QCM, thin films of the materials of interest were deposited on Quartz Crystals (QC), which were additionally equipped with Au layers below 100 nm thickness on both sides, enabling electrical contact. Bulk targets of W and EUROFER97 were used in a PREVAC magnetron sputtering system in Ar atmosphere using a gas flow rate of 10 standard cubic centimeter per minute (sccm), Ar pressure of  $5.5 \times 10^{-3}$  mbar, and a DC power of 50 W [22]. The use of EUROFER97 targets allowed to obtain films of comparable composition and crystallinity: A detailed characterization of films deposited from EUROFER97 using ion beam analysis is presented elsewhere [22,23]. The films of Fe were also deposited by magnetron sputtering as described elsewhere [24].

A QCM setup located at TU Wien was used to experimentally determine sputtering yield values during ion bombardment in ultrahigh vacuum (UHV) conditions. It allows to record mass changes in situ by measuring resonance frequency variations of a piezoelectrically excited quartz resonator disk [21]. In this setup, a high sensitivity to mass changes in the order of 10<sup>-4</sup> W monolayers per second can be achieved [25], which is realized by using special SC-cut quartz resonator disks and dedicated electronics. For the experiments, the covered side of the QCM, was then exposed to beams of different energies of D<sub>2</sub><sup>+</sup>, or He<sup>+</sup> ions delivered from a SPECS IQE 12/38 ion source. The generated ions were filtered according to their mass over charge ratio and the resulting ion beam was furthermore shaped and scanned in order to ensure a quasihomogeneous irradiation throughout the whole sensitive area of the QCM. Prior to each experiment, the samples were first sputter cleaned using Ar as projectile to remove potential contaminations that might have accumulated on the surface due to air expose. Additionally, the

samples were irradiated by  $D_2^+$  or  $He^+$  under normal incidence until stable conditions were reached. This pre-irradiation allowed to measure steady-state yields, i.e., erosion rates obtained after thermal equilibration and after initial implantation processes possibly occurring promptly after irradiation start, had saturated. The respective ion flux was determined by means of a Faraday cup before and after each measurement, ensuring steady ion irradiation. Both temporal as well as lateral fluctuations of the ion beam were considered for estimating the measurement error. The ion incidence angle was varied between  $0^\circ$  and  $70^\circ$  in the experiments in discrete angular steps of  $5^\circ$ , by tilting the sample relative to the ion beam via a motor-controlled goniometer. Due to the high sensitivity of the QCM, low ion fluxes could be employed, avoiding significant heating and unnecessary high fluences to the PFM/QCM sample. With information from both the mass loss and the ion flux, incidence-angle-dependent sputtering yields were calculated.

Atomic Force Microscopy (AFM) employing an Asylum Research Cypher S, were performed at ambient conditions before and after the sputtering yield measurements to ensure that the surfaces present low roughness and that ion beam exposure during the QCM measurements did not modify the surface morphologies. As an example, root mean square of roughness (Rq) values range from 1.088 to 1.092 nm for the W film on QCM before, and from 1.476 to 1.704 nm after sputtering yield measurements, without any significant change in morphological features. The low Rq observed by AFM indicates that no significant roughness effects are expected in the sputtering yield results [26,27].

SDTrimSP simulations [12] using a graphical user interface (GUI) developed at TU Wien were performed [28]. Such a GUI allows to easily apply corrections of different parameters to investigate its effects on sputtering yields compared to experimental data. For this study, amorphous flat surfaces of W, Fe, and EUROFER97 composition free of contaminants were considered as targets in the SDTrimSP sputtering yield simulations.

#### 3. Results and Discussion

#### 3.1. Electronic stopping power

Fig. 1 compiles recent measurements of electronic SCS for light ions in different PFM across a wide range of energies [17,29-33], while the magnified low-energy region is shown in Fig. 2. Commonly used semi empirical models from different versions of the Stopping and Range of Ions in Matter (SRIM-1997 and SRIM-2013) code [11,34] for electronic SCS, as well as the SCS calculated using the Lindhard-Scharff Formula for ions in the keV region [35] (available as inelastic energy loss model in the SDTrimSP code) are also presented for comparison. Good agreement between experimental SCS and SRIM-2013 can be observed for the case of H, D and He in W for medium (defined here as the region between 10-300 keV) and high energies (>1000 keV), as well as for H, D, and He in Fe for high energies. On the other hand, significant discrepancies are observed between experimental results and models: discrepancies around up to 11 % are observed around the maximum (Bragg peak) and 20 % for the low energy region around 5-10 keV for H, and D in Fe and EUROFER97 between experimental data and SRIM-2013. For the case of W, consistent discrepancies are observed between experimental data and SRIM-2013 for low energies, up to 60 % and 210 % for the case of He for SRIM-2013 and SRIM-1997, respectively.

It is unsurprising that discrepancies exist between semi-empirical models and recent experimental data, given the previously limited datasets available for light ions in W and Fe. Before 2021, the SCS database in W was limited to 4 datasets from 1972 to 1984 with energies ranging from 80 to 6000 keV for protons and 6 datasets from 1963 to 1974 with energies ranging from 300 to 19525 keV for He at the IAEA electronic stopping power database [36]. This scarcity of datasets, particularly at low energy regimes, reduces the accuracy of the empirical fits used in models. In addition, the simplest reasonable model system to describe energy transfer to the electronic system in the low energy

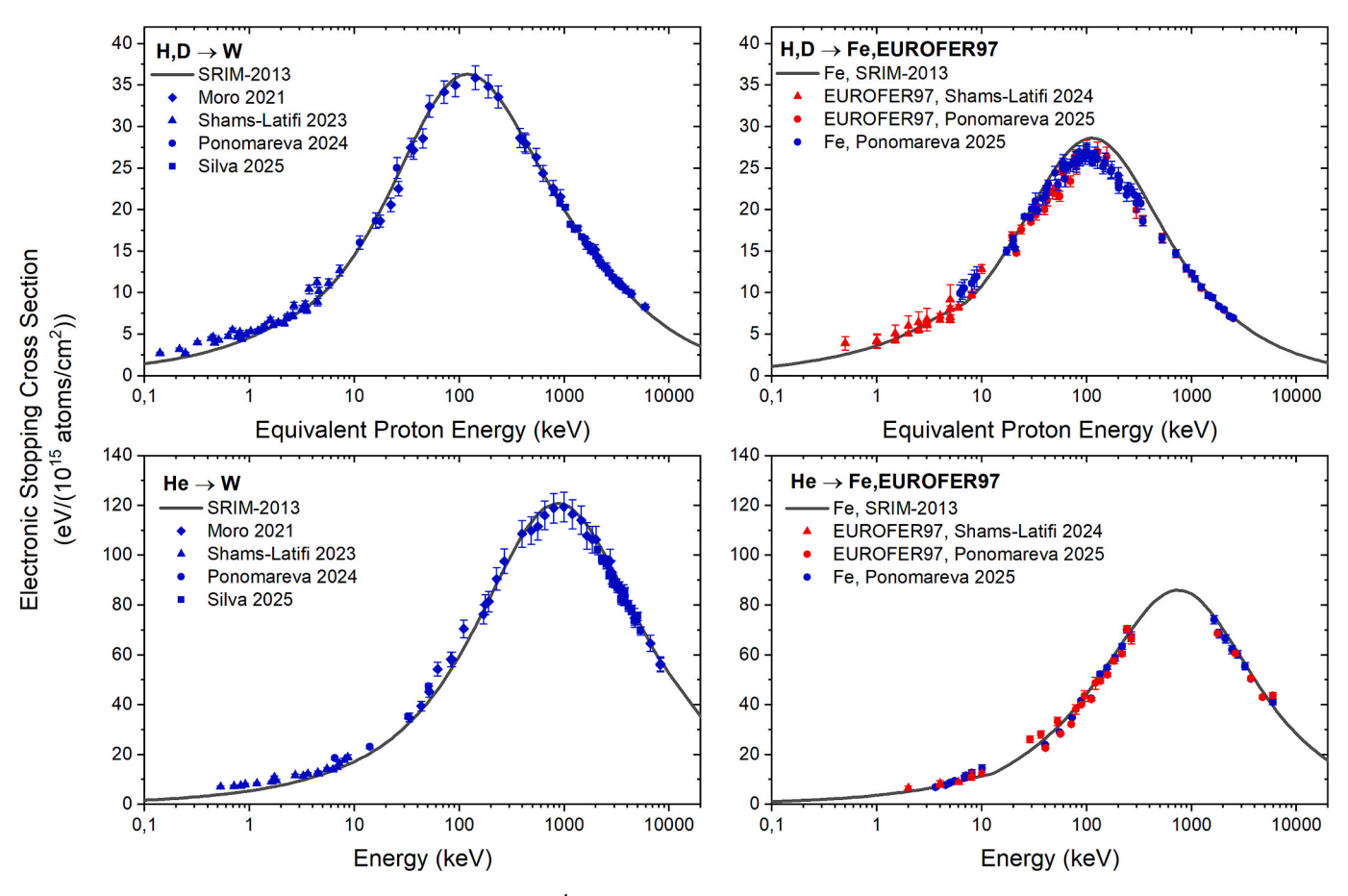


Fig. 1. SCS of W, Fe, and EUROFER97 for protons, deuterons and <sup>4</sup>He ions recently obtained experimentally from Moro [29], Shams-Latifi [17,31], Ponomoreva [30,32], and Silva [33]. Experimental results are compared to semi-empirical SCS from SRIM-2013 [34].

regimes is an ion moving in a free electron gas (FEG). This approach results in stopping power being velocity proportional [37], with a proportionality coefficient Q that depends on the atomic number of the projectile and the electron gas density. However, in the low-energy regime, several studies have reported limitations and deviations from the FEG model for different target materials [38,39]. These deviations are attributed to additional energy loss mechanisms, such as charge exchange effects during close ion-target encounters and excitation limits for specific ions at low energies.

#### 3.2. Interatomic potential

Repulsive interatomic potentials between ions and target atoms are critical in determining nuclear stopping power, scattering and recoil angle distribution, and the scattering and recoil cross-sections. Commonly used models considering screening by electrons in the low energy regime such as Ziegler-Biersack-Littmark (ZBL) [11] and Thomas-Fermi-Molière (TFM) [40] present significantly improved predictions compared to the Coulomb potential of bare nuclei. These models are, however, known to be inaccurate at low energies, and application of empirical correction factors  $(c_a)$  in the screening length (a) are recommended and result in further improvements of the model predictions [41]. Nevertheless, experimental reference data for several of ion-solid combinations remains scarce, and only recently the first experimental  $c_a$  for a PWI relevant combination at low energies was presented, derived from angular scans using low energy ion scattering in single-crystals [42]. Other interatomic models are proposed based on density function theory (DFT) calculations [43-45], which would benefit from validation based on experimental measurements.

Fig. 3 presents the backscattering yield of singly scattered ions

extracted from the surface peak for 3 keV primary He+ ions scattered under normal incidence from a W(110) single-crystal. Data is obtained experimentally throughout angular scans around the [010] crystal axis [42]. The observed angular pattern is a result from the shadow cone of surface layer atoms that block projectiles backscattered from deeper layers, in particular for this case the 2<sup>nd</sup> atomic layer from reaching the detector. Experimental results are compared to MD simulations using the software KALYPSO [46] considering different interatomic potentials: TFM with and without a ca correction of 0.85; ZBL, and the screened potential recently developed by Nordlund-Lehtola-Hobler (NLH) [45]. The difference between the models and the experimental data is also presented in Fig. 3, to better compare the best-fitting models with the experimental results. Clear discrepancies between uncorrected TFM and ZBL potentials and experimental results are observed in the width in the angular pattern. It is visible that applying a correction of 0.85 to the TFM potential significantly improves the simulation in comparison to the experimental results. Table 1 summarizes several ca for the TFM potential for He and D at 3 keV/atom in W and Fe [42]. One might notice that each correction represents a single combination of ionenergy-target, and its validity for different energies still needs to be investigated. On the other hand, simulations using the NLH potential also show good agreement with experimental results and highlight improvement in predicting the strength of the interatomic potential at low energies in comparison to TFM and ZBL potentials.

#### 3.3. Sputtering yield: Experimental and BCA simulations

The results of experimental SY for different ions and for redeposited PFM as a function of the incident angle are presented in Fig. 4. Comparable SY are obtained for both Fe and redeposited EUROFER97

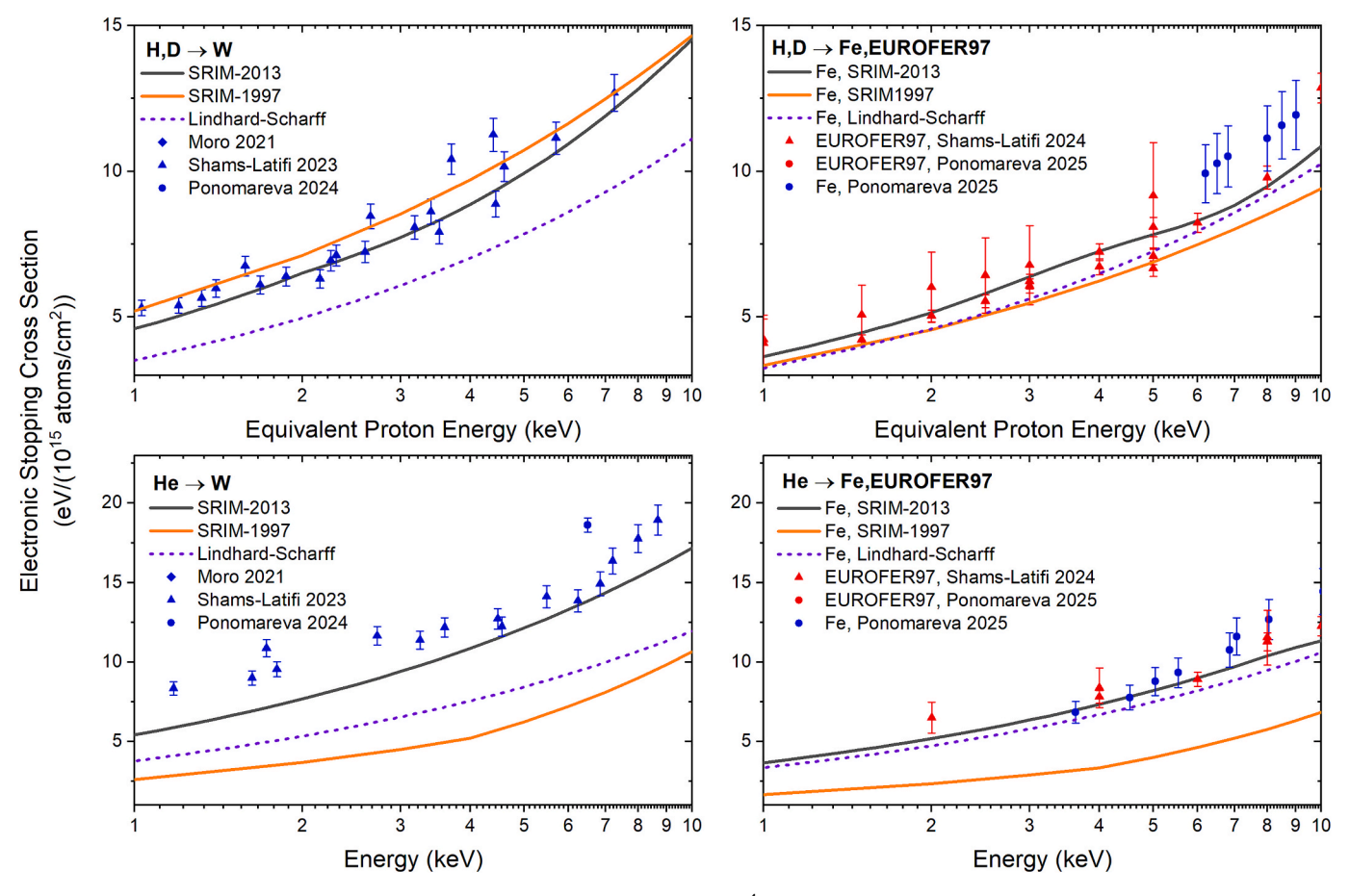


Fig. 2. SCS at low energies (≤10 keV) of W, Fe, and EUROFER97 for protons, deuterons ad <sup>4</sup>He ions recently obtained experimentally and compared to SRIM models as presented in Fig. 1. SCS from SRIM-1997 [11] and calculated using the Lindhard-Scharff formula for low velocity ions [35] are also presented for comparison.

(referred here as EUROFER97 for simplification) for all ions, as expected given the composition of 88.7 % of Fe atomic content in the films [22], and given the sufficiently low fluence used in the experiments which is expected not to induce significant changes in the composition of the films from preferential sputtering due to W surface enrichment [47,48]. Another feature in the experimental SY curves is observed between  $20^{\circ}$  to  $40^{\circ}$  incident angle, which is most pronounced for W and Fe films. This local minimum indicates the presence of a preferential crystal orientation in the films that can influence the sputtering yields for different incident angles [49,50]. This behavior is not observed to this extent for EUROFER97, suggesting no preferential crystal orientation on the surface.

SY simulations from SDTrimSP are presented for comparison to the experimental results in Fig. 5. The simulations were carried out using Lindhard-Scharf as inelastic energy loss model and TFM as interatomic potential model. These models were chosen because they allow straightforward application of empirical correction factors in SDTrimSP, enabling direct comparison with the experimentally derived SCS and ca values presented earlier in this work. While for the case of D<sub>2</sub>, c<sub>a</sub> was obtained at 3 keV/D, instead of the 1 keV/D investigated in the SY measurements, this correction is assumed to represent a significantly more accurate estimation than the uncorrected TFM potential. Across all ion-target combinations, the uncorrected SDTrimSP simulations consistently overestimate the experimental sputtering yields at all incident angles. In contrast, empirical corrections to both SCS and ca substantially reduces the discrepancies between simulation and experiment. However, even after applying corrections, notable discrepancies remain, particularly for D2 across all PFM studied. Despite measuring at steady state conditions, this difference may be partially attributed to mass gain from deuterium implantation in the films, which reduces the net mass

loss detected by the QCM. The effect of implantation is expected to scale with the penetration depth of the projectiles, thus rationalizing the larger discrepancy for D compared to He. A further, and potentially significant source of uncertainty lies in the crystallinity of the films. While the SDTrimSP simulations assume amorphous targets, the experimentally studied films exhibit polycrystalline structure with preferential orientation, as suggested by the angular dependence of the SY observed between 20° and 40°. Recent studies have demonstrated that sputtering yields in polycrystalline metals with randomly oriented grains can differ markedly from the SY of an amorphous material [51]. Grain orientation, channeling and texture effects in crystalline targets can all affect local sputter probabilities. Accurately accounting for these effects in BCA simulations remains challenging. Addressing this would require dedicated studies to quantify the effect, assisted by the continuous development of BCA simulation tools to incorporate empirically corrected parameters for different crystal orientations.

It is also worth noting that the surface binding energy, defined as the minimum energy required to remove an atom from the surface, is another input parameter that is often considered unknown and can significantly affect sputtering yield simulations [13,52]. Frequently, surface binding energy is treated as a free parameter to fit simulations to experimental data [53–55]. In this work, standard surface binding energy values from SDTrimSP were used.

Although the results summarized here significantly reduce the previous knowledge gap related to ion–solid interactions of slow, light ions in PFM, the need for further studies remains. Systematic investigations of interatomic potentials as a function of ion energy can help predict trends in how nuclear interactions occur at very low velocities. Similarly, expanding studies to other target materials may reveal clear trends across specific elemental groups, improving the predictability of

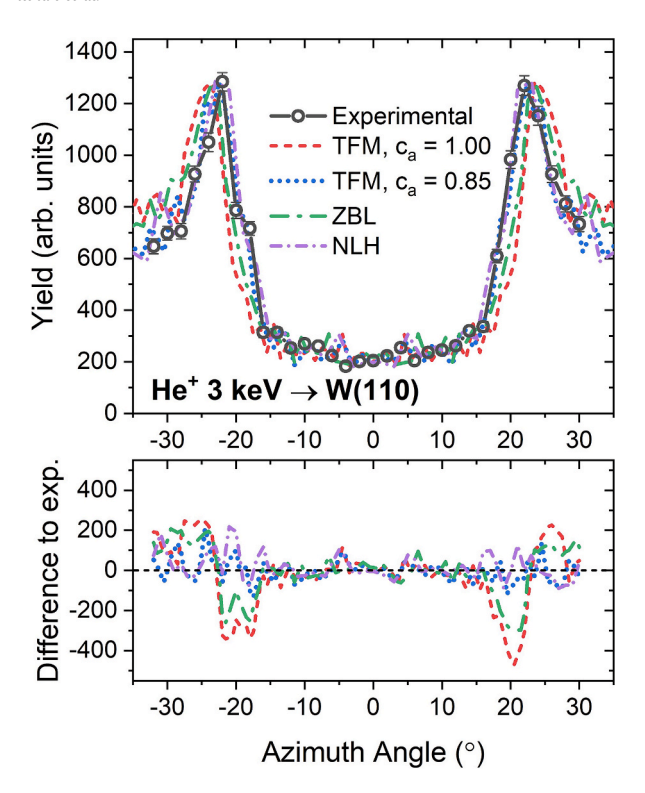


Fig. 3. Angular dependence of the surface scattering yield for  $3 \text{ keV He}^+$  from W(110) around the [010] crystal axis obtained experimentally [42] and compared to MD simulations using different potentials [45]. The difference between the different models and the experimental data is presented below.

Table 1 Empirical correction factors  $(c_a)$  for the TFM potential for different ions in W and Fe from [42].

Ion	c <sub>a</sub> (TFM) W(110)	Fe(100)
He <sup>+</sup> 3 keV	0.85	0.7
D <sub>2</sub> 3 keV/atom	0.95	≥0.85

ion–target combinations. Beyond the materials studied in this work, other fusion relevant materials, such as molybdenum (Mo) proposed for diagnostic mirrors [56,57], and boron (B), used for wall conditioning [3,58], also exhibit either scarce data or significant discrepancies in available datasets for electronic energy losses for light ions [36]. Additionally, the substantial presence of oxygen and hydrogen in PFM can induce changes in the electronic structure, affecting ion energy losses in ways not captured by simple Bragg's rule predictions [59,60], and highlights the need for specific studies in compound materials. Finally, there is no available experimental SCS in W and Fe for medium-Z ions, such as neon (Ne) and argon (Ar), proposed as seeding impurities in tokamaks [61,62]. These gases can significantly contribute to PFM erosion, underscoring the importance of expanding experimental efforts in this area.

#### 4. Summary and conclusion

This study reviewed the current status of available experimental data for electronic energy depositions and interatomic potentials for hydrogen isotopes and helium in W, Fe, and EUROFER97, comparing them with commonly used models. Significant discrepancies were identified in electronic stopping cross sections, particularly at low energies, with deviations reaching up to 210 %, depending on the selected energy loss model. Empirical correction factors for the TFM potential,

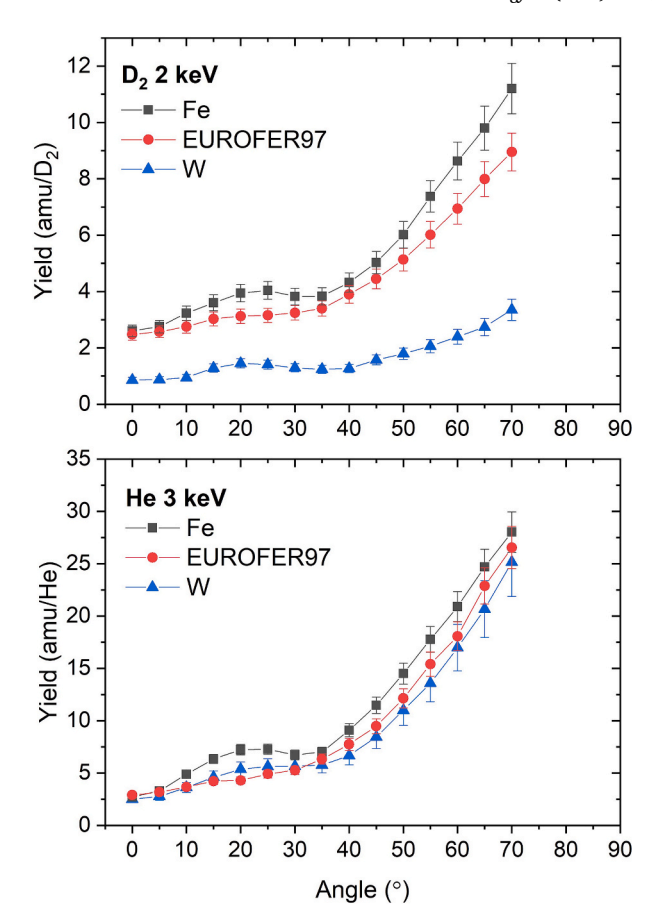


**Fig. 4.** Sputtering yields as a function of the ion incident angle, measured using a QCM system for the indicated ions and energies using redeposited films of Fe, EUROFER97, and W.

ranging from 0.7 to 0.95, were summarized, while recently developed potentials showed very good agreement with experimental data. Incorporating empirical corrections in SCS and adjusting interatomic potentials in BCA simulations of sputtering yields using the SDTrimSP code significantly reduced discrepancies between simulations and experimental sputtering data. The need for continued studies to better understand trends in the behavior of other fusion-relevant ions, targets, and energy ranges was identified, particularly for materials such as Mo and B, and for impurity seeding gases at low energies. These efforts will help to improve predictive capabilities for other ion–solid combinations, and enhance the accuracy of fundamental aspects related to plasma—wall interaction.

#### CRediT authorship contribution statement

E. Pitthan: Writing – original draft, Visualization, Validation, Supervision, Project administration, Methodology, Investigation, Funding acquisition, Formal analysis, Data curation, Conceptualization. M. Fellinger: Writing – review & editing, Visualization, Validation, Methodology, Investigation, Formal analysis, Data curation. B.Burazor Domazet: Writing – review & editing, Methodology, Investigation, Formal analysis. P.M. Wolf: Writing – review & editing, Methodology, Investigation, Formal analysis, Data curation. J. Shams-Latifi: Writing – review & editing, Investigation, Formal analysis, Data curation. F. Aumayr: Writing – review & editing, Supervision, Conceptualization. D. Primetzhofer: Writing – review & editing, Supervision, Resources, Funding acquisition, Data curation, Conceptualization.

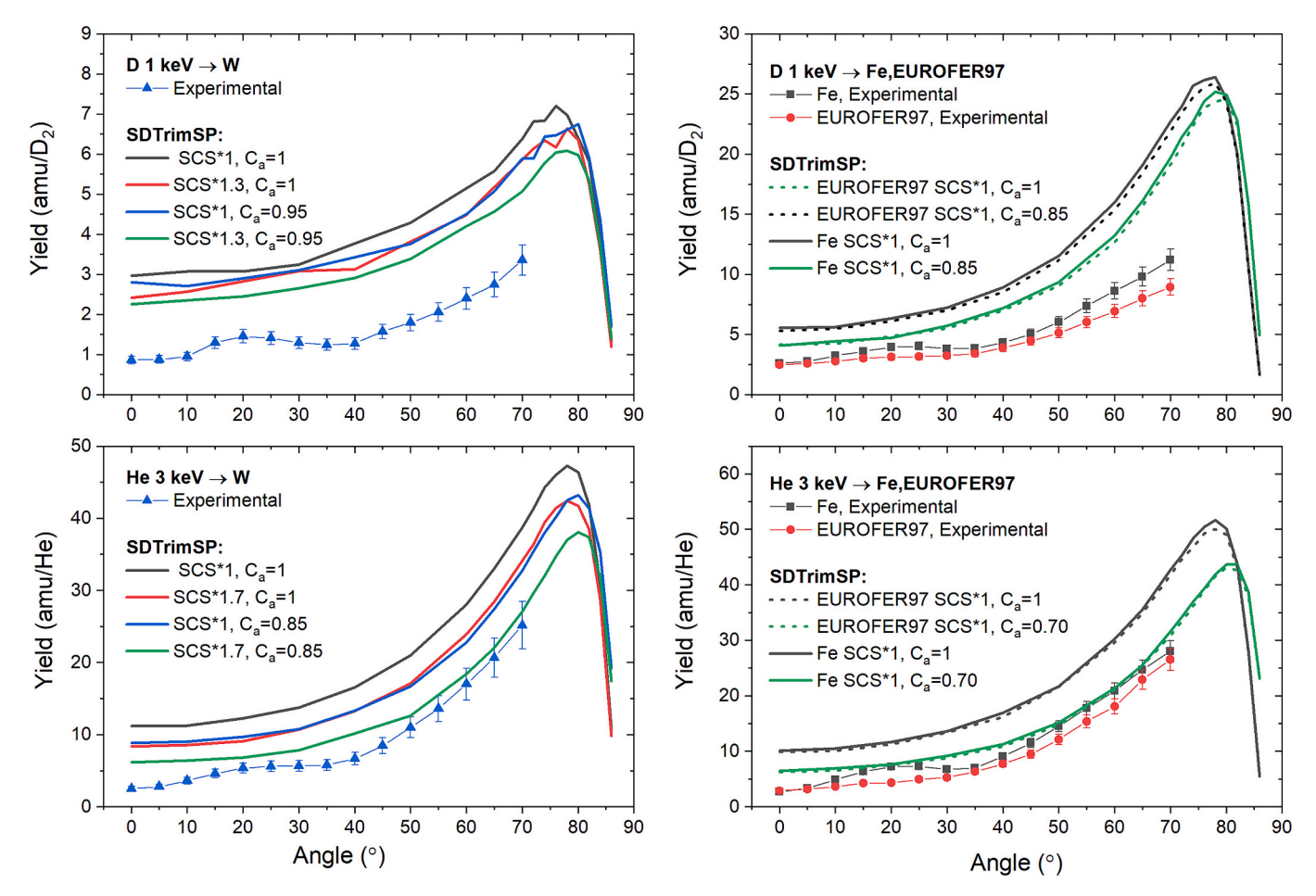


Fig. 5. Sputtering yields of D 1 keV and He 3 keV for W, Fe, and EUROFER97 simulated using SDTrimSP simulated for different incident angles with and without empirical corrections on SCS and  $c_a$  in comparison with the ones obtained experimentally.

#### Declaration of competing interest

The authors declare that they have no known competing financial interests or personal relationships that could have appeared to influence the work reported in this paper.

#### Acknowledgements

This work has been carried out within the framework of the EURO-fusion Consortium, funded by the European Union via the Euratom Research and Training Programme (Grant Agreement No 101052200 — EUROfusion). Views and opinions expressed are however those of the author(s) only and do not necessarily reflect those of the European Union or the European Commission. Neither the European Union nor the European Commission can be held responsible for them. Accelerator operation was supported by the Swedish Research Council VR-RFI, contracts #2019-00191 and #2023-00155, and the Swedish Foundation for Strategic Research (SSF) under contract RIF14-0053. This work was also supported by the Swedish Energy Agency (Grant No. P2023-01345). Financial support has also been provided by the Commission for the Coordination of Fusion Research in Austria (KKKÖ) at the Austrian Academy of Sciences (ÖAW).

#### Data availability

Data will be made available on request.

#### References

- S. Brezinsek, et al., Plasma-wall interaction studies within the EUROfusion consortium: progress on plasma-facing components development and qualification, Nucl. Fusion 57 (2017) 116041.
- [2] J.W. Coenen, M. Berger, M.J. Demkowicz, D. Matveev, A. Manhard, R. Neu, J. Riesch, B. Unterberg, M. Wirtz, Ch. Linsmeier, Plasma-wall interaction of advanced materials, Nucl. Mater. Energy 12 (2017) 307.
- [3] R.A. Pitts, A. Loarte, T. Wauters, M. Dubrov, Y. Gribov, F. Köchl, A. Pshenov, Y. Zhang, J. Artola, X. Bonnin, L. Chen, M. Lehnen, K. Schmid, R. Ding, H. Frerichs, R. Futtersack, X. Gong, G. Hagelaar, E. Hodille, J. Hobirk, S. Krat, D. Matveev, K. Paschalidis, J. Qian, S. Ratynskaia, T. Rizzi, V. Rozhansky, P. Tamain, P. Tolias, L. Zhang, W. Zhang, Plasma-wall interaction impact of the ITER re-baseline, Nucl. Mater. Energy 42 (2025) 101854.
- [4] K. Nordlund, S.J. Zinkle, A.E. Sand, F. Granberg, R.S. Averback, R.E. Stoller, T. Suzudo, F. Lorenzo Malerba, W.J. Banhart, F. Weber, S.L. Willaime, D. S. Dudarev, Primary radiation damage: a review of current understanding and models, J. Nucl. Mater. 512 (2018) 450.
- [5] J. Marian, C.S. Becquart, C. Domain, S.L. Dudarev, M.R. Gilbert, R.J. Kurtz, D. R. Mason, K. Nordlund, A.E. Sand, L.L. Snead, Recent advances in modeling and simulation of the exposure and response of tungsten to fusion energy conditions, Nucl. Fusion 57 (2017) 092008.
- [6] K. Nordlund, C. Björkas, T. Ahlgren, A. Lasa, A.E. Sand, Multiscale modelling of plasma-wall interactions in fusion reactor conditions, J. Phys. D Appl. Phys. 47 (2014) 224018.
- [7] H.H. Andersen, H.L. Bay, A survey of sputtering-yield data for plasma-wall interaction calculations, J. Nucl. Mater. 93 (1980) 625.
- [8] J. Bohdansky, Plasma contamination due to plasma -wall interaction, Phys. Scr. 23 (1981) 119.
- [9] T. Kawamura, Plasma—wall interaction and its effect on material selection, Fusion Eng. Des. 15 (1991) 1.
- [10] K. Ohya, Dynamic simulation of erosion and redeposition on plasma-facing materials, Phys. Scr. T124 (2006) 70.
- [11] J.F. Ziegler, J.P. Biersack, U. Littmark, The Stopping and Range of Ions in Solids, Volume I, Pergammon, New York, 1985.
- [12] A. Mutzke, R. Schneider, W. Eckstein, R. Dohmen, K. Schmid, U. von Toussaint, G. Badelow, SDTrimSP Version 6.00, IPP-Report 2019-02.

- [13] H. Hofsäss, K. Zhang, A. Mutzk, Simulation of ion beam sputtering with SDTrimSP, TRIDYN and SRIM, Applied Surface Science 310 (2014) 134.
- [14] A. Liptak, K.D. Lawson, M.I. Hasan, A molecular dynamics study of the sputtering processes of beryllium species by hydrogenic plasma, Sci. Rep. 15 (2025) 15065.
- [15] M. Kaufmann, R. Neu, Tungsten as first wall material in fusion devices, Fusion Eng. Des. 82 (2007) 521.
- [16] E. Gaganidze, F. Gillemot, I. Szenthe, M. Gorley, M. Rieth, E. Diegele, Development of EUROFER97 database and material property handbook, Fusion Eng. Des. 135 (2018) 9.
- [17] J. Shams-Latifi, E. Pitthan, P. Mika Wolf, D. Primetzhofer, Experimental electronic stopping cross-section of tungsten bulk and sputter-deposited thin films for slow protons, deuterons and helium ions, Nucl. Mater. Energy 36 (2023) 101491.
- [18] M. Mayer, S. Möller, M. Rubel, A. Widdowson, S. Charisopoulos, T. Ahlgren, E. Alves, G. Apostolopoulos, N.P. Barradas, S. Donnelly, Ion beam analysis of fusion plasma-facing materials and components: facilities and research challenges, Nucl. Fusion 60 (2019) 025001.
- [19] M. Rubel, D. Primetzhofer, P. Petersson, S. Charisopoulos, A. Widdowson, Accelerator techniques and nuclear data needs for ion beam analysis of wall materials in controlled fusion devices, EPJ Tech. Instrum. 10 (3) (2023) 1.
- [20] A. Widdowson, E. Alves, C.F. Ayres, A. Baron-Wiechec, S. Brezinsek, J.P. Coad, K. Heinola, J. Likonen, G.F. Matthews, M. Rubel, JET-EFDA contributors, Material migration patterns and overview of first surface analysis of the JET ITER-Like Wall, Phys. Scr. T159 (2014) 014010.
- [21] G. Hayderer, M. Schmid, P. Varga, H.P. Winter, F. Aumayr, A highly sensitive quartz-crystal microbalance for sputtering investigations in slow ion-surface collisions, Rev. Sci. Instrum. 70 (1999) 3696.
- [22] E. Pitthan, P. Petersson, T.T. Tran, D. Moldarev, R. Kaur, J. Shams-Latifi, P. Ström, M. Hans, M. Rubel, D. Primetzhofer, Thin films sputter-deposited from EUROFER97 in argon and deuterium atmosphere: Material properties and deuterium retention, Nucl. Mater. Energy 34 (2023) 101375.
- [23] J. Shams-Latifi, E. Pitthan, T.T. Tran, R. Kaur, D. Primetzhofer, Sputter-deposition of ultra-thin film stacks from EUROFER97 and tungsten: characterisation and interaction with low-energy D and He ions, Mater. Res. Express 11 (2024) 016518.
- [24] R. Stadlmayr, P.S. Szabo, B.M. Berger, C. Cupak, R. Chiba, D. Blöch, D. Mayer, B. Stechauner, M. Sauer, A. Foelske-Schmitz, M. Oberkofler, T. Schwarz-Selinger, A. Mutzke, F. Aumayr, Fluence dependent changes of surface morphology and sputtering yield of iron: Comparison of experiments with SDTrimSP-2D, Nucl. Instrum. Methods Phys. Res., Sect. B 430 (2018) 42.
- [25] A. Golczewski, K. Dobes, G. Wachter, M. Schmid, F. Aumayr, A quartz-crystal-microbalance technique to investigate ion-induced erosion of fusion relevant surfaces, Nucl. Instrum. Methods Phys. Res., Sect. B 267 (2009) 695.
- [26] M. Küstner, W. Eckstein, V. Dose, J. Roth, The influence of surface roughness on the angular dependence of the sputter yield, Nucl. Instrum. Methods Phys. Res., Sect. B 145 (1998) 320.
- [27] C. Cupak, P.S. Szabo, H. Biber, R. Stadlmayr, C. Grave, M. Fellinger, J. Brötzner, R. A. Wilhelm, W. Möller, A. Mutzke, M.V. Moro, F. Aumayr, Sputter yields of rough surfaces: Importance of the mean surface inclination angle from nanoto microscopic rough regimes, Appl. Surf. Sci. 570 (2021) 151204.
- [28] P.S. Szabo, D. Weichselbaum, H. Biber, C. Cupak, A. Mutzke, R.A. Wilhelm, F. Aumayr, Graphical user interface for SDTrimSP to simulate sputtering, ion implantation and the dynamic effects of ion irradiation, Nucl. Instrum. Methods Phys. Res., Sect. B 522 (2022) 47.
- [29] M.V. Moro, P.M. Wolf, B. Bruckner, F. Munnik, R. Heller, P. Bauer, D. Primetzhofer, Experimental electronic stopping cross section of tungsten for light ions in a large energy interval, Nucl. Instrum. Methods Phys. Res., Sect. B 498 (2021) 1.
- [30] E. Ponomareva, E. Pitthan, R. Holenák, J. Shams-Latifi, G. Pádraig Kiely, D. Primetzhofer, A.E. Sand, Local electronic excitations induced by low-velocity light ion stopping in tungsten, Phys. Rev. B 109 (2024) 165123.
- [31] J. Shams-Latifi, E. Pitthan, D. Primetzhofer, Experimental electronic stopping cross-section of EUROFER97 for slow protons, deuterons and helium ions, Radiat. Phys. Chem. 224 (2024) 112073.
- [32] E. Ponomareva, E. Pitthan, M.V. Moro, B. Bruckner, P. Bauer, F. Munnik, R. Heller, R. Nuñez Palacio, D. Primetzhofer, A.E. Sand, Role of alloying and defects in light ion energy dissipation in iron, Phys. Rev. B 112 (2025) 014313.
- [33] T. F. Silva, A. Silva, C. L. Rodrigues, N. Added, M. H. Tabacnika, F. Matias, H. Yoriyaz, J. Shorto, Electronic stopping cross sections of tungsten to swift ions and comparisons with models (submitted for publication).
- [34] J.F. Ziegler, M.D. Ziegler, J.P. Biersack, SRIM the stopping and range of ions in matter (2010), Nucl. Instrum. Methods Phys. Res., Sect. B 268 (2010) 1818.
- [35] J. Lindhard, M. Scharff, Energy Dissipation by Ions in the keV Region, Phys. Rev. 124 (1961) 128.
- [36] C.C. Montanari, P. Dimitriou, L. Marian, A.M.P. Mendez, J.P. Peralta, F. Bivort-Haiek, The IAEA electronic stopping power database: Modernization, review, and analysis of the existing experimental data, Nucl. Instrum. Methods Phys. Res., Sect. B 551 (2024) 165336.
- [37] E. Fermi, E. Teller, The capture of negative mesotrons in matter, Phys. Rev. 72 (1947) 399.

- [38] D. Roth, B. Bruckner, M.V. Moro, S. Gruber, D. Goebl, J.I. Juaristi, M. Alducin, R. Steinberger, J. Duchoslav, D. Primetzhofer, P. Bauer, Electronic Stopping of Slow Protons in transition and Rare Earth Metals: Breakdown of the Free Electron Gas Concept, Phys. Rev. Lett. 118 (2017) 103401.
- [39] D. Primetzhofer, S. Rund, D. Roth, D. Goebl, P. Bauer, Electronic Excitations of Slow Ions in a Free Electron Gas Metal: evidence for Charge Exchange Effects, Phys. Rev. Lett. 107 (2011) 163201.
- [40] G. Molière, Theorie der Streuung schneller geladener Teilchen I, Einzelstreuung am abgeschirmten Coulomb-Feld, Z. Naturforsch. A 2 (1947) 133.
- [41] D.J. O'connor, J.P. Biersack, Comparison of theoretical and empirical interatomic potentials, Nucl. Instrum. Methods Phys. Res., Sect. B 15 (1986) 14.
- [42] P.M. Wolf, E. Pitthan, D. Primetzhofer, Experimentally determined interatomic potentials in low-energy atomic collisions relevant for nuclear fusion, Phys. Rev. A 111 (2025) 042812.
- [43] M.A. Karolewski, Ab initio interatomic potentials for low energy He ion/atom scattering, Radiat Eff. Defects Solids 167 (2012) 666.
- [44] D.S. Meluzova, P.Y. Babenko, A.P. Shergin, K. Nordlund, A.N. Zinoviev, Reflection of hydrogen and deuterium atoms from the beryllium, carbon, tungsten surfaces, Nucl. Instrum. Methods Phys. Res., Sect. B 460 (2019) 4.
- [45] K. Nordlund, S. Lehtola, G. Hobler, Repulsive interatomic potentials calculated at three levels of theory, Phys. Rev. A 111 (2025) 032818.
- [46] M.A. Karolewski, Kalypso: a software package for molecular dynamics simulation of atomic collisions at surfaces, Nucl. Instrum. Methods Phys. Res., Sect. B 230 (2005) 402.
- [47] J. Roth, K. Sugiyama, V. Alimov, T. Höschen, M. Baldwin, R. Doerner, EUROFER as wall material: Reduced sputtering yields due to W surface enrichment, J. Nucl. Mater. 454 (2014) 1.
- [48] K. Sugiyama, J. Roth, V.K. Alimov, K. Schmid, M. Balden, S. Elgeti, F. Koch, T. Höschen, M.J. Baldwin, R.P. Doerner, H. Maier, W. Jacob, Erosion study of Fe–W binary mixed layer prepared as model system for RAFM steel, J. Nucl. Mater. 463 (2015) 272.
- [49] M. Balden, K. Schlueter, D. Dhard, P. Bauer, R. Nilsson, F. Granberg, K. Nordlund, G. Hobler, Crystal-orientation-dependent physical sputtering from four elemental metals, Nucl. Mater. Energy 37 (2023) 101559.
- [50] F. Kporha, K. Nordlund, F. Granberg, Sputtering of tungsten surfaces by different ion types: a molecular dynamics study, J. Nucl. Mater. 613 (2025) 155856.
- [51] K. Schlueter, K. Nordlund, G. Hobler, M. Balden, F. Granberg, O. Flinck, T.F. da Silva, R. Neu, Absence of a Crystal direction Regime in which Sputtering Corresponds to Amorphous Material, Phys. Rev. Lett. 125 (2020) 225502.
- [52] L.S. Morrissey, O.J. Tucker, R.M. Killen, S. Nakhla, D.W. Savin, Sputtering of surfaces by ion irradiation: a comparison of molecular dynamics and binary collision approximation models to laboratory measurements, J. Appl. Phys. 130 (2021) 013302.
- [53] N. Mahne, M. Cekada, M. Panjan, Total and Differential Sputtering yields Explored by SRIM Simulations. Coatings 12 (2022) 1541.
- [54] A. Farhadizadeh, T. Kozák, The importance of discharge voltage in DC magnetron sputtering for energy of sputtered and backscattered atoms on the substrate: Monte-Carlo simulations, Vacuum 196 (2022) 110716.
- [55] G. Sabiston, R.E. Wirz, Ion–surface interactions in plasma-facing material design, J. Appl. Phys. 135 (2024) 183301.
- [56] A. Litnovsky, M. Matveeva, A. Herrmann, V. Rohde, M. Mayer, K. Sugiyama, K. Krieger, V. Voitsenya, G. Vayakis, A.E. Costley, First studies of ITER-diagnostic mirrors in a tokamak with an all-metal interior: results of the first mirror test in ASDEX Upgrade, Nucl. Fusion 53 (2013) 073033.
- [57] L. Dittrich, P. Petersson, H. Laabadi, E. Pitthan, M. Rubel, A. Widdowson, A. Krawczyńska, K. Szlązak, Ł. Ciupiński, Impact of ion irradiation and film deposition on optical and fuel retention properties of Mo polycrystalline and single crystal mirrors, Nucl. Mater. Energy 37 (2023) 101548.
- [58] K. Schmid, T. Wauters, Full W ITER: Assessment of expected W erosion and implications of boronization on fuel retention, Nucl. Mater. Energy 41 (2024) 101789
- [59] P. Bauer, R. Golser, D. Semrad, P. Maier-Komor, F. Aumayr, A. Arnau, Influence of the chemical state on the stopping of protons and He-ions in some oxides, Nucl. Instrum. Methods Phys. Res., Sect. B 136 (1998) 103.
- [60] M. Brocklebank, S.N. Dedyulin, L.V. Goncharova, Stopping cross sections of protons in Ti, TiO<sub>2</sub> and Si using medium energy ion scattering, The European Physical Journal D 70 (2016) 248.
- [61] X. Zhao, C. Sang, Q. Zhou, C. Zhang, Y. Zhang, R. Ding, F. Ding, D. Wang, The erosion of tungsten divertor on EAST during neon impurity seeding in different divertor operation regimes, Plasma Phys. Control. Fusion 62 (2020) 055015.
- [62] A. Kumar, K. Shah, M.B. Chowdhuri, N. Ramaiya, A. Gauttam, K.A. Jadeja, B. Hedge, N. Yadava, K. Singh, S. Dolui, T. Macwan, A. Kumawat, P. Gautam, L. Pradhan, H. Raj, G. Shukla, D. Modi, S. Patel, S. Banerjee, I. Hoque, Komal, S. Aich, A. Patel, Utsav, A. Kanik, R. Kumar, P. Verma, K.M. Patel, K. Galodiya, M. Shah, R.L. Tanna, J. Ghosh, The effect of impurity seeding on edge toroidal rotation in the ADITYA-U tokamak, Nucl. Fusion 64 (2024) 086019.